Title:

Genetically-driven CD39 expression shapes human tumor-infiltrating CD8$^+$ T cell functions

Short title:

CD39 modulation improves tumor-infiltrating CD8 T cell functions

Authors:

Daniela Gallerano[1], Selina Ciminati[1], Alessio Grimaldi[1], Silvia Piconese[1-2], Ilenia Cammarata[1], Chiara Focaccetti[1], Ilenia Pacella[1], Daniele Accapezzato[1], Francesco Lancellotti[3], Luca Sacco[3], Roberto Caronna[3], Ombretta Melaiu[4-5], Doriana Fruci[4], Valentina D'Oria[6], Emy Manzi[7], Andrea Sagnotta[7], Chiara Parrino[7], Diego Coletta[7], Giovanna Peruzzi[8], Valentina Terenzi[9], Andrea Battisti[9], Andrea Cassoni[9], Maria Teresa Fadda[9], Stefania Brozzetti[10], Katia Fazi[10], Gian Luca Grazi[7], Valentino Valentini[9], Piero Chirletti[3], Antonella Polimeni[9], Vincenzo Barnaba[*1,2], Eleonora Timperi[#1].

Affiliations:

[1]Department of Internal Clinical, Anaesthesiologic and Cardiovascular Sciences, 00161, Rome, Italy.

[#]Current adress: INSERM U932, Institut Curie, PSL Research University, Paris, France

[2]Laboratory affiliated to Istituto Pasteur Italia-Fondazione Cenci-Bolognetti, Rome, Italy

[3]Dipartimento di Scienze Chirurgiche, "Sapienza" Università di Roma, Policlinico Umberto I, Rome, Italy.

This article has been accepted for publication and undergone full peer review but has not been through the copyediting, typesetting, pagination and proofreading process which may lead to differences between this version and the Version of Record. Please cite this article as doi: 10.1002/ijc.33131

[4]Department of Paediatric Haematology/Oncology and of Cell and Gene Therapy, Ospedale Pediatrico Bambino Gesù, IRCCS, 00146 Rome, Italy.

[5]Department of Biology, University of Pisa, 56126 Pisa, Italy.

[6]Confocal microscopy, Core Facility, Research Laboratories, Ospedale Pediatrico Bambino Gesù, IRCCS, 00146 Rome, Italy.

[7]HepatoBiliaryPancreatic Surgery IRCCS - Regina Elena National Cancer Institute, Rome, Italy.

[8]Center for Life Nano Science@Sapienza, Istituto Italiano di Tecnologia, 00161, Rome, Italy.

[9]Odontostomatogical and Maxillo-facial Sciences Department, Sapienza Università di Roma

[10]Dipartimento di Chirurgia "Pietro Valdoni", "Sapienza" Università di Roma, Policlinico Umberto I, Rome, Italy

*Corresponding author. E-mail address: vincenzo.barnaba@uniroma1.it (V. Barnaba).

Keywords: CD39, CD8$^+$ TILs, SNP, CD39 modulators, checkpoint inhibitors.

Novel and Impact (75 words)

In this study, by dissecting the mechanisms regulating the CD39 expression on tumor-infiltrating CD8$^+$ T cells, we provided evidence supporting that CD39 inhibition may represent a novel immunotherapy strategy.

Abbreviations:

CRC (colorectal cancer)

HNSCC (head and neck cancer)

ICB (immune check point blockade)

IF (Immunofluorescence)

mAbs (monoclonal antibodies)

NSCLC (non-small cell lung cancer)

N-TUM (non-tumor)

PBMC (peripheral blood mononuclear cells)

PCA (pancreatic cancer adenocarcinoma)

SNP (single nucleotide polymorphism)

TME (tumor microenvironment)

TRM (T resident memory)

TUM (tumor)

ABSTRACT 250 word (217)

In this study, we investigated the role of CD39 on tumor-infiltrating $CD8^+$ T lymphocytes ($CD8^+$ TILs) in colorectal, head and neck and pancreatic cancers. Partially confirming recent observations correlating the CD39 expression with T cell exhaustion, we demonstrated a divergent functional activity in $CD39^+CD8^+$ TILs. On the one hand, $CD39^+CD8^+$ TILs (as compared with their $CD39^-$ counterparts) produced significantly lower IFN-γ and IL-2 amounts, expressed higher PD-1, and inversely correlated with perforin and granzyme B expression. On the other, they displayed a significantly higher proliferative capacity *ex vivo* that was inversely correlated with the PD-1 expression. Therefore, $CD39^+CD8^+$ TILs,

including those co-expressing the CD103 (a marker of T resident memory [TRM] cells), were defined as partially dysfunctional T cells that correlate with tumor patients with initial progression stages. Interestingly, our results identified for the first time a single nucleotide polymorphism (SNP rs10748643 A > G), as a genetic factor associated with CD39 expression in $CD8^+$ TILs. Finally, we demonstrated that compounds inhibiting CD39-related ATPases improved $CD39^+CD8^+$ T cell effector function *ex vivo*, and that $CD39^+CD8^+$ TILs displayed effective suppression function *in vitro*. Overall these data suggest that the SNP analysis may represent a suitable predictor of $CD39^+CD8^+$ T cell expression in cancer patients, and propose the modulation of CD39 as a new strategy to restore partially exhausted $CD8^+$ TILs.

5000 words of text (5000)

INTRODUCTION

CD39 is a triphosphate diphosphohydrolase 1 (ENTPD1) enzyme expressed at high levels on the surface of cancer cells that, together with the enzymatic activity of CD73, is responsible of a cascade pathway, by which adenosine triphosphate (ATP) is converted in adenosine diphosphate (ADP) and cyclic adenosine monophosphate (cAMP), leading ultimately to the release of an immunosuppressive form of adenosine in the tumor microenvironment (TME) [1,2]. Adenosine is a signaling molecule that influences tumorigenesis directly via activation of adenosine receptors on tumor cells, affecting oncogenic processes of several solid human cancers [2–5]. However, recent observations

highlighted the expression of CD39 on different immune cells, playing diverse roles in cancer according to immune cell functions [6–12]. CD39 has been firstly described as a regulatory T cell (Treg) marker, whose activity is crucial to explicate immunosuppressive functions of Tregs degrading extracellular ATP [13]. CD39 expression on highly suppressive Tregs is controlled by a single nucleotide polymorphism (SNP-rs10748643) located in the promoter region of CD39, further modulating Treg suppressive functions [14,15]. Indeed, $CD39^+$ Tregs are accumulated in different solid cancers supporting the suppression of anti-tumor immune responses [7,16,17].

More recent evidences proposed the expression of CD39 on $CD8^+$ T cells as a marker of exhausted tumor-infiltrating lymphocytes (TILs), in both a variety of experimental tumor models [18,19] and human solid cancers (e.g., non-small cell lung cancer [NSCLC], colorectal cancer [CRC] and head and neck cancer [HNSCC]) [20–22], in which the exhausted phenotype was characterized by low ability of IFN-γ production and high expression of PD1 [20–22]. Despite the majority of these data described $CD39^+CD8^+$ T cells as exhausted $CD8^+$ T cells in tumors, a recent study demonstrated the co-expression of CD39 with the CD103 marker of resident memory $CD8^+$ T cells (TRM), suggesting a protective role for these cells in cancer survival [23–25].

Our study analyzed the frequency of $CD39^+CD8^+$ TILs in various human solid tumors (i.e., CRC, HNSCC, pancreatic cancer adenocarcinoma [PCA]) and showed a functional dichotomy of these cells (poor IFN-γ production and cytotoxic activity *vs.* enhanced proliferation). In addition, it described for the first time the role of a single nucleotide polymorphism modulating CD39 expression on $CD8^+$ TILs, and supported the possibility that

CD39 expression may represent a valid biomarker of partially exhausted $CD8^+$ TILs, and even a novel immune checkpoint for restoring T cell exhaustion [26,27]. Given the importance of $CD8^+$ TILs in solid cancers and their impact on cancer survival [28], and because the current checkpoint inhibitors (e.g. ant-PD-1, anti-CTLA-4, anti-PDL-1 monoclonal antibodies [mAbs]) are not efficient for all tumor types or cause partial remission in the majority of tumors [29–32], innovative immunotherapy strategies particularly based on the combination of different approaches including new inhibitors providing immune check point blockade (ICB) [33–35], can strongly impact the phenotypic and functional features of $CD8^+$ T cells in the TME.

MATERIALS AND METHODS

Human samples and processing

Peripheral blood mononuclear cells (PBMCs), tumor (TUM) and non-tumor (N-TUM) surgery specimens were obtained from patients enrolled at the Policlinico Umberto I, Sapienza University of Rome and at the Istituto Nazionale dei Tumori, Regina Elena, Rome, upon approval by the Institutional Ethic Committee (No. 3596, 4382, 2926). All procedures were performed in accordance with the ethical standards of the 1975 Helsinki declaration and its amendments and with the patients' informed consent.

The study included patients with CRC (n=60), HNSCC (n=19), PCA (n=3) and a patient with NSCLC on Nivolumab treatment (followed up by 3 time points; each treatment has been performed every 21 days). CRC patients were not previously treated with adjuvant chemotherapy. Patient characteristics are listed in Table S1 and S2.

PBMCs were isolated from the patients' fresh blood by density gradient centrifugation with Lympholyte (Cedarlane Cat# CL502) and collected in complete RPMI 1640 medium (Gibco Cat# 22409-015) containing 10% FBS (Gibco Cat# 10270-106), 2 mM L-glutamine (Gibco Cat# 25030-024), penicillin/streptomycin (Sigma Cat# 15070-063), non-essential amino acids (Aurogene Cat# AU-X0557-100), Na-pyruvate (Euroclone Cat# ECM0160009), and 50 mM 2-mercaptoethanol (Sigma Cat# M6250).

Mononuclear cells (MCs) were isolated from TUM and N-TUM tissue optimizing a published protocol [7,35]. Tissue specimens were washed in HBSS Ca-Mg- (Gibco Cat# 14175-095), 1mM DTT (Sigma Aldrich Cat# D0632-25G), 2,5% FBS (Gibco Cat# 10270-106) 15min at 37°C, and in PBS (Sigma Aldrich Cat# D8537), 0.75mM EDTA (Sigma Aldrich Cat# E4884) 2x15min at 37°C. Tissue disruption was achieved by mechanical and enzymatic dissociation on a GentleMACS dissociator (MACS C tubes, Miltenyi Cat# 130-096-334), in HBSS Ca+Mg+ (Gibco Cat# 14025-050), 0.5mg/ml Collagenase IV (Sigma Aldrich Cat# C5138), 50ng/ml DNAseI (Worthington Cat# LS002058), 6mg/ml BSA (Sigma Aldrich Cat# A9418), 2% FBS (Gibco Cat# 10270-106), pre-warmed at 37°C, performing two dissociation cycles at RT, 116 rpm, 36" and one cycle at 37°C, 20 rpm, 10min. The enzymatic digestion was blocked with cold HBSS Ca-Mg- and specimens were filtered through a 70um cell strainer. Isolated cells were pelleted by centrifugation (1600rpm 10min), washed in 40% Percoll (GE Healthcare Cat# GE17-0891-01) and MCs were recovered by density gradient separation (as above), washed in PBS and collected in complete RPMI medium.

Flow cytometry

Multicolor flow cytometry was performed using antibodies listed in Table S3 and following latest guidelines for flow cytometry studies [36]. Dead cells were excluded using fixable Viability Dye eFluor™780 (eBioscience Cat# 65-0865-14) 30min at room temperature. Surface staining was performed incubating cells with antibodies 20min at 4°C in PBS 2% FBS. Intracellular staining was achieved using Fix/Perm and Perm-Wash buffers according to manufacturer's instructions (BD Cat# 554714, eBioscience Cat# 00-5523-00). Before T-bet, cytokine and Ki67 staining, cells were stimulated 4h at 37°C with Cell Stimulation Cocktail plus protein transport inhibitors (eBioscience Cat# 00-4975-03). Data were acquired on LSR Fortessa (BD) and analysed with FlowJo software (LLC, version 10.2). For the gating strategy, lymphocytes were selected based on SSC-A and FSC-A, doublets excluded using FSC-A and FSC-H. CD8 T cells were gated as live cells staining negative for dump gate markers identifying non-T cell lineages (CD14, CD16, CD19 and CD56) and negative for CD4.

SNP analysis

For CD39 SNP genotyping, DNA was extracted from patient PBMCs (1-5 x10^6 cells) using the DNeasy Blood and Tissue kit (Qiagen Cat# 69504) and quantified on an Implen P330 nanophotometer. Analysis of the SNP (rs10748643) in the *ENTPD1* gene (Chr10:97516764) was performed with the specific TaqMan SNP Genotyping assay (Applied Biosystems Cat# 4351379) [14,15] on 10ng DNA/sample following manufacturer instructions. Real-Time PCR was performed on a StepOne instrument (Applied Biosystems).

Immunofluorescence analysis

Immunofluorescence (IF) staining was performed on 2μm formaldehyde-fixed paraffin embedded (FFPE) serial tissue sections following deparaffinization and antigen retrieval procedures. Slides were blocked for 60 min with 1% BSA and 5% normal goat serum and antibodies were added consecutively [37] as follows. First, sections were incubated with anti-CD103 antibody overnight at 4°C, followed by 60 min incubation with Alexa Fluor 488 goat anti-rabbit IgG. Then, slides were incubated with Alexa Fluor® 594 anti-human CD39 antibody for 2 hours at RT, followed by 40 min incubation with mouse IgG and then 60 min with Alexa Fluor 647 anti-CD8 (Table S4). After staining, slides were counterstained with Hoechst (H3570, Invitrogen) for 5 min and coverslipped with 60% glycerol in PBS. Confocal microscopy imaging was performed by Leica TCS-SP8X laser-scanning confocal microscope (Leica Microsystems) equipped with tunable white light laser source, 405 nm diode laser, 3 (PMT) e 2 (HyD) internal spectral detector channels. Sequential confocal images were acquired using a HC PLAPO 40x oil immersion objective (1.30 numerical aperture, Leica Microsystems) with a 1024 × 1024 image format, scan speed 400 Hz. The density of $CD103^+$, $CD39^+$ and $CD8^+$ cells was recorded, as the number of positive cells per unit tissue surface area (mm^2). The mean, by two blinded examiners, of positive cells detected in 5 fields for each sample was used in the statistical analysis.

CFSE analysis

To evaluate proliferative capacity, PB, N-TUM and TUM MCs were labeled for 15 min with CFSE (Life Technologies Cat# C34554) and stimulated with anti-CD3/anti-CD28 Dynabeads (Gibco Cat# 11131D) at a ratio 1:4 in complete medium at 37°C for 7 days. Cells were then stained for flow cytometry analysis as described above and CFSE dilution was

analyzed in gated $CD8^+$ T cells. The experiment was performed in 5 independent analyses, for three patients with colorectal cancer and two patients with pancreatic cancer.

Suppression assay

To evaluate the suppressive capacity of $CD39^+$ $CD8^+$ T cells, total PBMCs from different healthy donors (HDs) were cultured for 4 days with anti-CD3 and anti-CD28 beads (Invitrogen), ratio 1:1. At day 4 CD39 expression has been checked by FACS analysis and donors with higher percentage of $CD39^+$ $CD8^+$ T cells were selected for sorting. $CD39^+$ and $CD39^-$ CD8 T cell counterparts were sorted by using a FACSAria III (BD Biosciences) equipped with Near UV 375, 488 and 633 nm laser and the FACSDiva software (version 6.1.3; BD Biosciences). The sorting panel included CD3, CD8, CD39 markers and Live-dead. Data were analyzed using the FlowJo software (TreeStar, USA). As gate strategy, lymphocytes were gated for FSC-A and SSC-A and doublets excluded using both FSC-A and H and SSC-A and H, after that live $CD8^+$ T cells ($CD3^+$/$CD8^+$ and Live-dead eFluor780$^-$ cells) were sorted as $CD39^+$ or $CD39^-$ cells. Following isolation, an aliquot of the collected cells was evaluated for purity at the same sorter resulting in an enrichment >99% for $CD39^+$ and $CD39^-$ $CD8^+$ T cells counterparts. The suppression assay has been performed culturing $CD39^+$ and $CD39^-$ sorted cells, labelled with eF670 (eBioscience cell proliferation dye) together with autologous PBMCs (targets) labelled with CFSE (cell proliferation tracker), at different ratios. As control, autologous PBMCs were cultured alone. At day 4, the percentage of CFSE-diluting $CD4^+$ T cells has been estimated by FACS analysis, and the percentage of $CD4^+$ T cell inhibition has been calculated, according the following formula: %inhibition = (%CFSE-stained $CD4^+$ T cells with $CD39^+$ $CD8^+$ T cells – CFSE-stained $CD4^+$ T cells

without $CD39^+$ $CD8^+$ T cells) / (%CFSE-stained $CD4^+$ T cells without $CD39^+$) x 100. The experiments were repeated 3 times, independently, including 4 donors for each experiment, analysed in triplicates.

CD39 inhibition assay

In vitro inhibition assays were performed on PBMCs isolated from fresh blood of HDs (N=4). *Ex vivo* assays were performed on MCs from PB, N-TUM and TUM from 5 colorectal cancer and 2 pancreatic cancer patients for a total of 7 independent experiments that gave similar results. In both *in vitro* and *ex vivo* assays, cells were plated ($2x10^5$ cells/well) and stimulated with anti-CD3/anti-CD28 Dynabeads (Gibco Cat# 11131D) at a ratio 1:4 for 4 days at 37°C. Cells were then treated with the CD39 inhibitor Polyoxotungstate-1 (POM-1) (20, 50 µM, R&D Systems Cat# 2689) once per day for 7 consecutive days. Cells were washed and stained for flow cytometry as described above.

Statistical analyses

Statistical analysis was performed using Prism software (version 7.0, GraphPad). Mann–Whitney test, 2-tailed, Wilcoxon matched-pairs test, 2-tailed, paired matched t-test, 2-tailed were applied to compare groups of FC *ex vivo* analysis. Two-way-ANOVA test (Tukey's multiple comparison test) has been applied for *in vitro* and *ex vivo* CD39 inhibition experiments with POM compounds. $P<0.05$ was considered statistically significant in all tests. Correlations were calculated using the nonparametric Spearman's correlation test, two-tailed.

RESULTS

Tumor-infiltrating CD39^{high}CD8^{+} T cells correlate with initial tumor stages and co-express the CD103 TRM marker

We first evaluated the expression of CD39 on CD8^{+} T cells derived from PB, N-TUM and TUM surgery specimens in different solid cancers, by multiparametric flow cytometry (FC). By calculating the levels of CD39 expression as CD39^{high} and CD39^{dim}, we found that both CD39^{high} and CD39^{dim} CD8^{+} T cells were significantly more represented in N-TUM and TUM than in PB, and that the CD39^{high} were significantly more represented in TUM than in N-TUM, in both CRC and HNSCC patients (Figure 1A-C). A similar hierarchy was observed by calculating the level of CD39^{+} CD8^{+} T cells infiltrating TUM or N-TUM, without discriminating CD39^{high} and CD39^{dim} cells (data not shown). The accumulation of CD39^{+}CD8^{+} T cells in TUM was also confirmed in both CRC and HNSCC tissues by IF (Suppl. Figure 1A, B).

To better characterize the CD39^{+}CD8^{+} T cell phenotype, we evaluated the expression of CCR7 and CD45RA discriminating naïve (N; CCR7^{+}CD45RA^{+}), central memory (CM; CCR7^{+}CD45RA^{-}), effector memory (TEM; CCR7^{-}CD45RA^{-}), and effector memory CD45RA^{+} (TEMRA; CCR7^{-}CD45RA^{+}) cells [38]. The majority of CD39^{+}CD8^{+} T cells were confined within the CD8^{+} TEM cell subset, in all PB, N-TUM and TUM districts of CRC patients, with a special representation in the TUM district (Suppl. Figure 1C). In addition, we analyzed the expression of nuclear transcription factors T-box (T-bet) and Eomesodermin (Eomes), helping to discriminate functional T-bet^{+}Eomes^{+} and dysfunctional T-bet^{-}Eomes^{+} CD8^{+} T cells, on the basis of previous experimental data showing that T-bet (key transcription factor of IFN-γ) expression is associated with the control of chronic infections

or tumors through the down-regulation of the exhaustion marker PD-1, and that Eomes expression characterizes dysfunctional memory $CD8^+$ T cells when it is not co-expressed with T-bet . The majority of $CD39^+CD8^+$ T cells in N-TUM and TUM contained similar frequencies of effector $Tbet^+Eomes^+$ and dysfunctional $Tbet^-Eomes^+$ $CD8^+$ T cells (Suppl. Fig. 1D), suggesting a balance between $Tbet^+$ and $Eomes^+$ cell proportions within $CD39^+CD8^+$ T cell subsets. In particular, the percentages of $Tbet^+$ and $Eomes^+$ cells were almost similar within $CD39^+CD8^+$ T cells or $CD39^-CD8^+$ T cells, proposing that CD39 does not seem to correlate with the Eomes or T-bet expression (Suppl. Fig. 1D) [20]. To correlate the $CD39^+CD8^+$ T cell frequency with the clinical outcome, we assessed the distribution of $CD39^{high}CD8^+$ T cells among the progression stages of CRC or HNSCC. $CD39^{high}CD8^+$ T cells were significantly or tended to be more accumulated in TUM of both CRC and HNSCC patients with initial progression stages (I-II) than in those with advanced stages of cancer (III-IV) (Figure 1D, E), supporting the hypothesis that $CD39^+CD8^+$ T cells may harbor a protective role during cancer progression [20,21]. Moreover, $CD39^+$ T cells were significantly accumulated within $CD8^+$ T cells co-expressing the marker of tissue resident memory T cells (TRM), CD103, in both N-TUM and TUM districts (Suppl. Fig. 2A, B). These data were confirmed by IF analysis revealing triple positive $CD8^+CD39^+CD103^+$ T cells to be accumulated in TUM at higher levels than N-TUM CRC (Suppl. Fig. 2C).

CD39 is shaped by genetic contribution of single nucleotide polymorphism (rs10748643)

We next investigated the genetic background of CD39 expression on $CD8^+$ TILs. In particular we verified the possibility that CD39 expression on $CD8^+$ TILs may be associated

with the SNP, rs10748643 (A > G) within the *ENTPD1* gene [14,15,39], that was shown to modulate CD39 expression on Tregs [7,14,15]. PCR-based SNP rs10748643 A > G analysis on PBMCs of CRC patients, highlighted that GG homozygous patients showed the highest frequencies of $CD39^+CD8^+$ T cells in N-TUM and TUM districts, as compared with patients with AA and AG variants (Figure 2A). These data were partially confirmed by counting $CD39^+CD8^+$ T cells in cancer tissues by IF (Suppl. Fig. 3A). Considering the limitation of IF, we could not discriminate the intensity level of $CD39^{high}$ or $CD39^{dim}$ expression as by FC. The difference in expression levels between allelic variants could be observed for the $CD39^{high}CD8^+$ T cell subset (Figure 2B) but not for the $CD39^{dim}CD8^+$ T cell subset (Suppl. Fig. 3B). These findings suggest that the SNP rs10748643 A > G contributes in determining CD39 levels in cancer-associated $CD8^+$ T cells. To test the possibility that the SNP rs10748643 A > G may influence CD39 levels upon T cell receptor (TCR) activation, we monitored CD39 expression in PBMCs from HDs with various allelic CD39 variants following a polyclonal TCR stimulus with anti-CD3/anti-CD28 *in vitro*. Notably, after 4 days, only homozygous GG individuals were able to significantly upregulate CD39 expression, as compared with the AA homozygous or the AG heterozygous individuals (Figure 2C). These findings propose for the first time the pivotal role of genetic imprinting on CD39 expression levels in $CD8^+$ T cells. Interestingly, the rs10748643 A > G SNP also impacted on the accumulation of $CD8^+CD39^+CD103^+$ triple positive cells: indeed, AG and GG patients contained much more $CD8^+CD39^+CD103^+$ cells in TUM compared to N-TUM districts, quantified by both FC (data not shown) and IF, further supporting a strong impact of the genetic factor in shaping $CD39^+$ cells in CRC cancer patients (Figure 2D).

CD39^{+}CD8^{+} T cells display divergent functional capacities

To understand the role of CD39 expression on TILs, we studied the CD39^{+}CD8^{+} functional capacities. FC analyses showed that CD39^{+}CD8^{+} T cells expressing high levels of PD-1 were especially enriched in TUM samples, as compared with N-TUM and PB of both CRC (Figure 3A, B) and in HNSCC patients (Suppl. Fig. 4A, B). In addition, PD-1 expression was significantly more represented among CD39^{high}, than among CD39^{dim} T cells infiltrating TUM districts in both CRC (Figure 3C) and HNSCC (Suppl. Fig. 4C), suggesting a predisposition of CD39^{high}CD8^{+} TILs to express the highest levels of PD-1. In concordance with these data, the percentage of CD39^{+}CD8^{+} T cells positively correlated with the percentage of PD-1^{+}CD8^{+} T cells in TUM districts of both CRC (Figure 3D) and HNSCC patients (Suppl. Fig. 4D). In order to evaluate whether PD-1 overexpression was effectively related with T cell exhaustion, we checked the capacity of CD39^{+}CD8^{+} T cells to produce IFN-γ, to express cytotoxicity-related molecules, and to proliferate *ex vivo*. The percentage of IFN-γ^{+} cells elicited in response to phorbol 12-myristate 13-acetate- Ionomycin (PMA-IONO) brefeldin A- monensin (BFA-MONO) stimulation, was significantly lower within CD39^{+}CD8^{+} T cells than within CD39^{-}CD8^{+} T cells, particularly in the TUM compartment (Figure 3E). Parallelly, the percentage of CD39^{+}CD8^{+} T cells inversely correlated with the percentage of CD8^{+} T cells expressing cytotoxicity-related molecules, such as Granzyme B and Perforin (Figure 3F-G). Interestingly, when we analyzed CD8^{+} T cell responses in the context of anti-PD1 therapy, in a NSCLC patient on Nivolumab treatment, we observed that upon PD-1-blockade, CD39^{-}PD-1^{+}CD8^{+} T cells increased their capacity to produce IFN-γ *ex vivo*, more that the CD39^{+}PD-1^{+}CD8^{+} T cells (Figure 3H). This observation suggests that co-expression

of CD39 and PD-1 marks a $CD8^+$ T cell subset with a deeper dysfunction in terms of IFN-γ production, and that, anti-PD1 treatment may restore IFN-γ production only by $PD1^+CD8^+$ T cells not expressing CD39.

Preliminary data showed a relationship between SNP rs10748643 (A > G) and some markers of T cell dysfunction (i.e., PD-1 overexpression and granzyme B/perforin downregulation), tested in the entire $CD8^+$ population (Suppl. Fig. 3C-D). Consistent with the seminal observation describing $CD103^+CD39^+CD8^+$ T cells as exhausted TRM cells [21], $CD103^+CD39^+$ TILs produced less IFN-γ and IL-2, expressed PD-1 at a significant higher extent than the $CD103^+CD39^-$ subset (Figure 4A), and directly correlated with $PD1^+CD8^+$ cells (Figure 4B). Taken together, these data support a negative impact of the genetically-shaped CD39 on both type-1 response and cytotoxic markers during cancer responses, and that CD39 marks a subset of $CD103^+CD8^+$ TRM with dysfunctional type-1 response and cytotoxic properties.

To further investigate the effect of CD39/PD-1 co-expression, we studied the proliferative capacity of $CD8^+$ TILs expressing PD-1 and/or CD39 in CRC patients, by analyzing the CFSE dilution within these T cell subsets from PBMCs, N-TUM- and TUM-derived MCs, after 7 days of TCR stimulation with anti-CD3/anti-CD28 (Figure 5A). In contrast with the results obtained by IFN-γ production, $CD39^-PD\text{-}1^+CD8^+$ T cells proliferated at a significantly lesser extent than $CD39^+PD\text{-}1^+$ cells and even lesser than $CD39^+PD\text{-}1^-$ cells isolated from both N-TUM and TUM districts (Figure 5A-B). These results were highlighted by data retrieved in the NSCLC patient on anti-PD-1 treatment. FC analysis of peripheral $CD8^+$ T cells at baseline and at different time points during therapy showed that the percentage of

$CD39^+CD8^+$ T cells progressively increased during anti-PD-1 therapy (Figure 5C). More important, the highest levels of $ki67^+$ proliferative cells were observed within the $CD39^+PD\text{-}1^+CD8^+$ T cell subset, as compared with the $CD39^-PD\text{-}1^+$ or $CD39^+PD\text{-}1^-$ subsets, and increased even more upon anti-PD-1 therapy (Figure 5C).

CD39 marks suppressor $CD8^+$ T cells

On the basis of previous evidence showing that CD39 provides strong suppressive capacity to tumor-infiltrating $CD4^+FOXP3^+$ Tregs [16,40], we tested the potential suppressive capacity of $CD8^+$ T cells expressing CD39 *in vitro*. For this purpose, we observed the effect of co-culturing CFSE-labelled PBMCs, as targets, with decreasing concentrations of sorted autologous $CD39^+$ or $CD39^-$ $CD8^+$ T cells, as effectors (1:1, 1:2, 1:4, 1:8, 1:16, 1:32, 1:64). Since the amount of $CD39^+$ cells isolated from TUM districts were too low for the suppression assay, we used PBMCs from 4 HDs with the GG SNP-genotype (particularly prone to upregulate CD39 expression on $CD8^+$ T cells, see Fig. 2C) upon upregulation of CD39 expression by TCR stimulus. Notably, the percentage of CFSE-diluting $CD4^+$ T cells was reduced when PBMCs were co-cultured with decreasing concentrations of $CD39^+CD8^+$ T cells significantly more than when co-cultured with parallel concentrations of $CD39^-CD8^+$ T cells (Fig. 5D). As a consequence, the percentage of inhibition of CFSE-diluting $CD4^+$ T cells supported that sorted $CD39^+CD8^+$ T cells were able to suppress $CD4^+$ T cell proliferation (Figure 5E). These data highlight the possibility that CD39 expression on $CD8^+$ T cells contributes in establishing the suppressive $CD8^+$ T cell capacity that, together with genetic factors, can shift the balance of T cell effector/suppressive activity in TME.

CD39 inhibition restores CD8 T cell functions

We next aimed to study the role of CD39 as exhaustion marker, by analyzing the blocking effect on the CD39 pathway of $CD8^+$ T cells by the Polyoxotungstate-1 (POM) compound, known to inhibit the ecto-ATPases (i.e. NTPDase1, NTPDase2, NTPDase3 and NPP1) [4,8]. First, we evaluated if T cell activation (in terms of percentage of $CD25^+$ cells) or functions (in terms of both IFNγ production and cytotoxic activity, as detected by CD107a expression) were improved in the presence of POM inhibitor, upon 4-day stimulation of PBMCs (derived from HDs) with anti-CD3/anti-CD28 *in vitro*. Interestingly, at day 4, in the presence of POM, a significant increase of both CD25 percentage and effector functions was detected only within $CD39^+CD8^+$ T cells (Figure 6A). Conversely, the $CD39^-$ counterparts did not show any change, suggesting a direct POM-mediated $CD39^+CD8^+$ T cell targeting.

To further explore the possibility of CD39 inhibition in cancer settings, we set up an assay blocking CD39 activity with POM compound *ex vivo*, using peripheral, TUM or N-TUM $CD8^+$ T cells from cancer patients. $CD8^+$ TILs from both CRC and PCA patients, showed a significant increase of CD107a expression upon POM-conditioned stimulation, and a significant downregulation of PD-1 expression in both N-TUM- and TUM-derived $CD8^+$ T cells, evaluated as both percentage and MFI (Figure 6B-D). Interestingly, the CD107a overexpression resulted significantly evident upon the POM-conditioned stimulation in both $CD39^+PD1^+$ and $CD39^+PD1^-CD8^+$ subsets, but not in $CD39^-PD1^+CD8^+$ cells (Figure 6E), suggesting a specific POM activity on $CD39^+CD8^+$ TIL portion. Taken together, the results suggest that the CD39 inhibition shifts the balance of $CD8^+$ T cells towards a functional effector phenotype, with a concomitant downregulation of PD-1 expression.

DISCUSSION

Our data firstly, confirmed that human solid tumors – in particular CRC and HNSCC – are characterized by a population of $CD8^+$ TILs expressing the ectonucleotidase CD39 at high level ($CD39^{high}$), often in association with CD103 that marks $CD8^+$ TRM cells [20,21]. $CD39^+CD8^+$ TILs were particularly enriched during the initial stages of CRC and HNSCC cancer progression and declined in advanced stages. This data is consistent with recent observations showing that CD39 expression particularly when associated with CD103, identifies tumor-reactive TILs and results as a prognostic survival factor in human solid tumors [20,21 23–25].

The genetic background of CD39 expression on $CD8^+$ TILs allowed us to give a possible explanation to the wide variability of CD39 expression patterns [20], despite a study on a larger cohort of patients is required to validate this association. Indeed, we found that the rs10748643 A > G SNP in the *ENTPD1* gene, which was shown to play a role in CD39 expression on Tregs [7,14,15], was associated with CD39 upregulation also on $CD8^+$ TILs (including the $CD8^+CD39^+CD103^+$ TRM cells) *ex vivo*, as well as on peripheral $CD8^+$ T cells upon TCR stimulus *in vitro*. Thus, a relevant impact of CD39 expression on $CD8^+$ T cells is played by the genetic background of the patients, in addition with the environmental factors [21,41].

Collectively, our data indicate that $CD39^+CD8^+$ TILs including $CD39^+PD\text{-}1^+CD103^+$ TRM cells, display a split functional capacity, whereby they could potentially compensate the dysfunctions in IFN-γ production and killing activity, by the capability to proliferate more

extensively, to counteract tumor progression in the TME. As consequence, the PD-1 blockade therapy resulted in restoring IFN-γ production by $CD39^{-}PD1^{+}CD8^{+}$ T cells, and in enhancing proliferative capacity by $CD39^{+}PD\text{-}1^{+}CD8^{+}$ T cells [42]. On the other hand, $CD39^{+}CD8^{+}$ T cells showed a consistent suppressive capacity, that is basically instrumental to avoid excessive tissue damage during chronic inflammatory diseases, but that, in the long-term, can favor cancer development or progression. This is in line with reports describing CD39 as a suppressive marker on $CD4^{+}$ Tregs [13], and with a recent work showing CD39 involved in suppression exerted by $CD8^{+}$ Tregs [43].

At the mechanistic level, it remains unclear how CD39 expression levels can translate into the divergent functions, poor IFN-γ production and killing capacity *vs.* enhanced proliferation, as well as high suppression capacity. Further studies are required both to ascertain whether the CD39-driven generation of adenosine delivers the negative signals providing poor IFN-γ production and killing capacity [44], and to dissect possible paths capable to (directly or indirectly) deliver signals promoting enhanced proliferation into $CD39^{+}CD8^{+}$ T cells, or suppression capacity. Whatever the mechanism(s) whereby $CD39^{+}CD8^{+}$ T cells display their peculiar and contrasting effects (diminished IFN-γ production, decreased killing capacity, enhanced proliferation, acquisition of suppression function), they may represent a partially exhausted cell population that may be potentially susceptible to be rescued by compounds inhibiting the negative signals provided by CD39. This hypothesis was supported by our results showing that a selective inhibitor of the ecto-ATPases (POM) [8,32] both enhanced activation and effector functions of peripheral $CD39^{+}CD8^{+}$ T cells *in vitro* and

$CD39^+CD8^+$ TILs *ex vivo*, in relation with PD-1 down-regulation, and significantly reduced their suppression function (data not shown).

In sum, our data strongly emphasize the divergent functions of $CD39^+CD8^+$ T cells suggesting that further studies are required to dissect these functions at single cell level, in order to identify novel molecular signatures that might be considered potential strategies for cancer immunotherapy [6,45,46]. In addition, the correlation of rs10748643 A > G SNP with CD39 expression on $CD8^+$ T cells favors the clinical application of this SNP analysis, not only as a prognostic marker of cancer progression, but also as a predictive tool for the response to novel immune-checkpoint therapeutic approaches targeting $CD39^+CD8^+$ TILs in human cancers.

Acknowledgements

We thank Flavia Longo for NSCLC samples included in the study. This work was supported by the following grants: Associazione Italiana per la Ricerca sul Cancro (AIRC) (progetti "Investigator Grant" [IG]-2014-17 id. 15199 and IG-2017-22 id. 19939 to VB; and IG-2017-22 id. 19784 to SP; and IG-2016-20 id. 18495 to DF; The Accelerated Award 2018 (Project Id.22794 to VB); Fondazione Italiana Sclerosi Multipla (FISM) Call_2019 (cod. 2019/R-Single/053 to VB); Istituto Pasteur Italia – Fondazione Cenci Bolognetti (grant 2014-2016 to SP); International Network Institut Pasteur, Paris – "Programmes Transversaux De Recherche" (PTR n. 20-16 to SP and VB). C.F. was supported by a post-doctoral fellowship of the Fondazione Veronesi (2015). D.G. and O.M. were supported by a post-doctoral fellowship of the Fondazione Veronesi (2017). E.T. was supported by a post-doctoral fellowship abroad of the AIRC (2018/2020- number:20934).

Disclosure of Potential Conflicts of Interest

No potential conflicts of interest were disclosed.

Data accessibility

The data that support the findings of this study are available from the corresponding author upon reasonable request.

References 50 (46)

1. Di Virgilio F, Sarti AC, Falzoni S, De Marchi E, Adinolfi E. Extracellular ATP and P2 purinergic signalling in the tumour microenvironment. *Nat Rev Cancer [Internet]* 2018 [cited 2020 Mar 3];18:601–18. Available from: http://www.nature.com/articles/s41568-018-0037-0

2. Stagg J, Smyth MJ. Extracellular adenosine triphosphate and adenosine in cancer. *Oncogene [Internet]* 2010 [cited 2020 Mar 3];29:5346–58. Available from: http://www.nature.com/articles/onc2010292

3. Aliagas E, Vidal A, Texidó L, Ponce J, Condom E, Martín-Satué M. High Expression of Ecto-Nucleotidases CD39 and CD73 in Human Endometrial Tumors. *Mediators of Inflammation [Internet]* 2014 [cited 2020 Mar 9];2014:1–8. Available from: http://www.hindawi.com/journals/mi/2014/509027/

4. Bastid J, Regairaz A, Bonnefoy N, Dejou C, Giustiniani J, Laheurte C, Cochaud S, Laprevotte E, Funck-Brentano E, Hemon P, Gros L, Bec N, et al. Inhibition of CD39

Enzymatic Function at the Surface of Tumor Cells Alleviates Their Immunosuppressive Activity. *Cancer Immunology Research [Internet]* 2015 [cited 2020 Mar 3];3:254–65. Available from: http://cancerimmunolres.aacrjournals.org/cgi/doi/10.1158/2326-6066.CIR-14-0018

5. Stella J, Bavaresco L, Braganhol E, Rockenbach L, Farias PF, Wink MR, Azambuja AA, Barrios CH, Morrone FB, Oliveira Battastini AM. Differential ectonucleotidase expression in human bladder cancer cell lines. *Urologic Oncology: Seminars and Original Investigations [Internet]* 2010 [cited 2020 Mar 9];28:260–7. Available from: https://linkinghub.elsevier.com/retrieve/pii/S1078143909000362

6. Allard B, Longhi MS, Robson SC, Stagg J. The ectonucleotidases CD39 and CD73: Novel checkpoint inhibitor targets. *Immunol Rev [Internet]* 2017 [cited 2020 Mar 3];276:121–44. Available from: http://doi.wiley.com/10.1111/imr.12528

7. Timperi E, Pacella I, Schinzari V, Focaccetti C, Sacco L, Farelli F, Caronna R, Del Bene G, Longo F, Ciardi A, Morelli S, Vestri AR, et al. Regulatory T cells with multiple suppressive and potentially pro-tumor activities accumulate in human colorectal cancer. *Oncoimmunology* 2016;5:e1175800.

8. Zhang H, Vijayan D, Li X-Y, Robson SC, Geetha N, Teng MWL, Smyth MJ. The role of NK cells and CD39 in the immunological control of tumor metastases. *OncoImmunology [Internet]* 2019 [cited 2020 Mar 3];8:e1593809. Available from: https://www.tandfonline.com/doi/full/10.1080/2162402X.2019.1593809

9. Ryzhov SV, Pickup MW, Chytil A, Gorska AE, Zhang Q, Owens P, Feoktistov I, Moses HL, Novitskiy SV. Role of TGF-β Signaling in Generation of CD39 $^{+}$ CD73 $^{+}$ Myeloid Cells in Tumors. *JI [Internet]* 2014 [cited 2020 Mar 3];193:3155–64. Available from: http://www.jimmunol.org/lookup/doi/10.4049/jimmunol.1400578

10. Borsellino G, Kleinewietfeld M, Di Mitri D, Sternjak A, Diamantini A, Giometto R, Höpner S, Centonze D, Bernardi G, Dell'Acqua ML, Rossini PM, Battistini L, et al. Expression of ectonucleotidase CD39 by Foxp3+ Treg cells: hydrolysis of extracellular ATP and immune suppression. *Blood* 2007;110:1225–32.

11. Montalbán del Barrio I, Penski C, Schlahsa L, Stein RG, Diessner J, Wöckel A, Dietl J, Lutz MB, Mittelbronn M, Wischhusen J, Häusler SFM. Adenosine-generating ovarian cancer cells attract myeloid cells which differentiate into adenosine-generating tumor associated macrophages – a self-amplifying, CD39- and CD73-dependent mechanism for tumor immune escape. *j immunotherapy cancer [Internet]* 2016 [cited 2020 Mar 9];4:49. Available from: http://jitc.bmj.com/lookup/doi/10.1186/s40425-016-0154-9

12. Fang F, Yu M, Cavanagh MM, Hutter Saunders J, Qi Q, Ye Z, Le Saux S, Sultan W, Turgano E, Dekker CL, Tian L, Weyand CM, et al. Expression of CD39 on Activated T

Cells Impairs their Survival in Older Individuals. *Cell Reports [Internet]* 2016 [cited 2020 Mar 9];14:1218–31. Available from: https://linkinghub.elsevier.com/retrieve/pii/S2211124716000061

13. Deaglio S, Dwyer KM, Gao W, Friedman D, Usheva A, Erat A, Chen J-F, Enjyoji K, Linden J, Oukka M, Kuchroo VK, Strom TB, et al. Adenosine generation catalyzed by CD39 and CD73 expressed on regulatory T cells mediates immune suppression. *J Exp Med* 2007;204:1257–65.

14. Rissiek A, Baumann I, Cuapio A, Mautner A, Kolster M, Arck PC, Dodge-Khatami A, Mittrücker H-W, Koch-Nolte F, Haag F, Tolosa E. The expression of CD39 on regulatory T cells is genetically driven and further upregulated at sites of inflammation. *J Autoimmun* 2015;58:12–20.

15. Timperi E, Folgori L, Amodio D, De Luca M, Chiurchiù S, Piconese S, Di Cesare S, Pacella I, Martire C, Bonatti G, Perrone S, Boni T, et al. Expansion of activated regulatory T cells inversely correlates with clinical severity in septic neonates. *J Allergy Clin Immunol* 2016;137:1617-1620.e6.

16. Ahlmanner F, Sundström P, Akeus P, Eklöf J, Börjesson L, Gustavsson B, Lindskog EB, Raghavan S, Quiding-Järbrink M. $CD39^{+}$ regulatory T cells accumulate in colon adenocarcinomas and display markers of increased suppressive function. *Oncotarget [Internet]* 2018 [cited 2020 Mar 3];9. Available from: http://www.oncotarget.com/fulltext/26435

17. Park Y-J, Ryu H, Choi G, Kim B-S, Hwang ES, Kim HS, Chung Y. IL-27 confers a protumorigenic activity of regulatory T cells via CD39. *Proc Natl Acad Sci USA [Internet]* 2019 [cited 2020 Mar 3];116:3106–11. Available from: http://www.pnas.org/lookup/doi/10.1073/pnas.1810254116

18. Canale FP, Ramello MC, Núñez N, Furlan CLA, Bossio SN, Serrán MG, Boari JT, del Castillo A, Ledesma M, Sedlik C, Piaggio E, Gruppi A, et al. CD39 Expression Defines Cell Exhaustion in Tumor-Infiltrating $CD8^{+}$ T Cells. *Cancer Res [Internet]* 2018 [cited 2020 Mar 3];78:115–28. Available from: http://cancerres.aacrjournals.org/lookup/doi/10.1158/0008-5472.CAN-16-2684

19. Canale FP, Ramello MC, Núñez N, Bossio SN, Piaggio E, Gruppi A, Rodríguez EVA, Montes CL. CD39 Expression Defines Cell Exhaustion in Tumor-Infiltrating CD8+ T Cells-Response. *Cancer Res* 2018;78:5175.

20. Simoni Y, Becht E, Fehlings M, Loh CY, Koo S-L, Teng KWW, Yeong JPS, Nahar R, Zhang T, Kared H, Duan K, Ang N, et al. Bystander CD8+ T cells are abundant and phenotypically distinct in human tumour infiltrates. *Nature* 2018;557:575–9.

21. Duhen T, Duhen R, Montler R, Moses J, Moudgil T, de Miranda NF, Goodall CP, Blair TC, Fox BA, McDermott JE, Chang S-C, Grunkemeier G, et al. Co-expression of CD39 and CD103 identifies tumor-reactive CD8 T cells in human solid tumors. *Nat Commun* 2018;9:2724.

22. Gupta PK, Godec J, Wolski D, Adland E, Yates K, Pauken KE, Cosgrove C, Ledderose C, Junger WG, Robson SC, Wherry EJ, Alter G, et al. CD39 Expression Identifies Terminally Exhausted CD8+ T Cells. *PLoS Pathog* 2015;11:e1005177.

23. Edwards J, Wilmott JS, Madore J, Gide TN, Quek C, Tasker A, Ferguson A, Chen J, Hewavisenti R, Hersey P, Gebhardt T, Weninger W, et al. CD103 $^{+}$ Tumor-Resident CD8 $^{+}$ T Cells Are Associated with Improved Survival in Immunotherapy-Naïve Melanoma Patients and Expand Significantly During Anti–PD-1 Treatment. *Clin Cancer Res [Internet]* 2018 [cited 2020 Mar 3];24:3036–45. Available from: http://clincancerres.aacrjournals.org/lookup/doi/10.1158/1078-0432.CCR-17-2257

24. Djenidi F, Adam J, Goubar A, Durgeau A, Meurice G, de Montpréville V, Validire P, Besse B, Mami-Chouaib F. CD8 $^{+}$ CD103 $^{+}$ Tumor–Infiltrating Lymphocytes Are Tumor-Specific Tissue-Resident Memory T Cells and a Prognostic Factor for Survival in Lung Cancer Patients. *JI [Internet]* 2015 [cited 2020 Mar 3];194:3475–86. Available from: http://www.jimmunol.org/lookup/doi/10.4049/jimmunol.1402711

25. Komdeur FL, Prins TM, van de Wall S, Plat A, Wisman GBA, Hollema H, Daemen T, Church DN, de Bruyn M, Nijman HW. CD103+ tumor-infiltrating lymphocytes are tumor-reactive intraepithelial CD8+ T cells associated with prognostic benefit and therapy response in cervical cancer. *Oncoimmunology* 2017;6:e1338230.

26. Pauken KE, Wherry EJ. SnapShot: T Cell Exhaustion. *Cell [Internet]* 2015 [cited 2020 Mar 10];163:1038-1038.e1. Available from: https://linkinghub.elsevier.com/retrieve/pii/S0092867415014105

27. Wherry EJ, Kurachi M. Molecular and cellular insights into T cell exhaustion. *Nat Rev Immunol* 2015;15:486–99.

28. Topalian SL, Taube JM, Anders RA, Pardoll DM. Mechanism-driven biomarkers to guide immune checkpoint blockade in cancer therapy. *Nat Rev Cancer* 2016;16:275–87.

29. Borghaei H, Paz-Ares L, Horn L, Spigel DR, Steins M, Ready NE, Chow LQ, Vokes EE, Felip E, Holgado E, Barlesi F, Kohlhäufl M, et al. Nivolumab versus Docetaxel in Advanced Nonsquamous Non-Small-Cell Lung Cancer. *N Engl J Med* 2015;373:1627–39.

30. Okazaki T, Chikuma S, Iwai Y, Fagarasan S, Honjo T. A rheostat for immune responses: the unique properties of PD-1 and their advantages for clinical application. *Nat Immunol* 2013;14:1212–8.

31. Sharma P, Allison JP. The future of immune checkpoint therapy. *Science* 2015;348:56–61.

32. Topalian SL, Hodi FS, Brahmer JR, Gettinger SN, Smith DC, McDermott DF, Powderly JD, Carvajal RD, Sosman JA, Atkins MB, Leming PD, Spigel DR, et al. Safety, activity, and immune correlates of anti-PD-1 antibody in cancer. *N Engl J Med* 2012;366:2443–54.

33. Schinzari V, Timperi E, Pecora G, Palmucci F, Gallerano D, Grimaldi A, Covino DA, Guglielmo N, Melandro F, Manzi E, Sagnotta A, Lancellotti F, et al. Wnt3a/β-Catenin Signaling Conditions Differentiation of Partially Exhausted T-effector Cells in Human Cancers. *Cancer Immunol Res* 2018;6:941–52.

34. Pacella I, Cammarata I, Focaccetti C, Miacci S, Gulino A, Tripodo C, Ravà M, Barnaba V, Piconese S. Wnt3a Neutralization Enhances T-cell Responses through Indirect Mechanisms and Restrains Tumor Growth. *Cancer Immunol Res* 2018;6:953–64.

35. Timperi E, Focaccetti C, Gallerano D, Panetta M, Spada S, Gallo E, Visca P, Venuta F, Diso D, Prelaj A, Longo F, Facciolo F, et al. IL-18 receptor marks functional CD8+ T cells in non-small cell lung cancer. *Oncoimmunology* 2017;6:e1328337.

36. Cossarizza A, Chang H-D, Radbruch A, Acs A, Adam D, Adam-Klages S, Agace WW, Aghaeepour N, Akdis M, Allez M, Almeida LN, Alvisi G, et al. Guidelines for the use of flow cytometry and cell sorting in immunological studies (second edition). *Eur J Immunol* 2019;49:1457–973.

37. Cammarata I, Martire C, Citro A, Raimondo D, Fruci D, Melaiu O, D'Oria V, Carone C, Peruzzi G, Cerboni C, Santoni A, Sidney J, et al. Counter-regulation of regulatory T cells by autoreactive CD8+ T cells in rheumatoid arthritis. *J Autoimmun* 2019;99:81–97.

38. Geginat J, Lanzavecchia A, Sallusto F. Proliferation and differentiation potential of human CD8+ memory T-cell subsets in response to antigen or homeostatic cytokines. *Blood* 2003;101:4260–6.

39. Friedman DJ, Künzli BM, A-Rahim YI, Sevigny J, Berberat PO, Enjyoji K, Csizmadia E, Friess H, Robson SC. From the Cover: CD39 deletion exacerbates experimental murine colitis and human polymorphisms increase susceptibility to inflammatory bowel disease. *Proc Natl Acad Sci USA* 2009;106:16788–93.

40. Fletcher JM, Lonergan R, Costelloe L, Kinsella K, Moran B, O'Farrelly C, Tubridy N, Mills KHG. CD39 $^{+}$ Foxp3 $^{+}$ Regulatory T Cells Suppress Pathogenic Th17 Cells and Are Impaired in Multiple Sclerosis. *J Immunol [Internet]* 2009 [cited 2020 Mar 3];183:7602–10. Available from: http://www.jimmunol.org/lookup/doi/10.4049/jimmunol.0901881

41. Raczkowski F, Rissiek A, Ricklefs I, Heiss K, Schumacher V, Wundenberg K, Haag F, Koch-Nolte F, Tolosa E, Mittrücker H-W. CD39 is upregulated during activation of mouse and human T cells and attenuates the immune response to Listeria monocytogenes. *PLoS ONE* 2018;13:e0197151.

42. Yost KE, Satpathy AT, Wells DK, Qi Y, Wang C, Kageyama R, McNamara KL, Granja JM, Sarin KY, Brown RA, Gupta RK, Curtis C, et al. Clonal replacement of tumor-specific T cells following PD-1 blockade. *Nat Med* 2019;25:1251–9.

43. Parodi A, Battaglia F, Kalli F, Ferrera F, Conteduca G, Tardito S, Stringara S, Ivaldi F, Negrini S, Borgonovo G, Simonato A, Traverso P, et al. CD39 is highly involved in mediating the suppression activity of tumor-infiltrating CD8+ T regulatory lymphocytes. *Cancer Immunol Immunother* 2013;62:851–62.

44. Vigano S, Alatzoglou D, Irving M, Ménétrier-Caux C, Caux C, Romero P, Coukos G. Targeting Adenosine in Cancer Immunotherapy to Enhance T-Cell Function. *Front Immunol [Internet]* 2019 [cited 2020 Mar 3];10:925. Available from: https://www.frontiersin.org/article/10.3389/fimmu.2019.00925/full

45. Lerner AG, Kovalenko M, Welch M, Cruz T dela, Jones J, Wong C, Spatola B, Eberhardt M, Wong A, Fung W, Lagpacan L, Losenkova K, et al. Abstract 5012: Targeting CD39 with a first-in-class inhibitory antibody prevents ATP processing and increases T-cell activation [Internet]. In: Immunology. American Association for Cancer Research, 2019 [cited 2020 Mar 3]. 5012–5012.Available from: http://cancerres.aacrjournals.org/lookup/doi/10.1158/1538-7445.AM2019-5012

46. Perrot I, Michaud H-A, Giraudon-Paoli M, Augier S, Docquier A, Gros L, Courtois R, Déjou C, Jecko D, Becquart O, Rispaud-Blanc H, Gauthier L, et al. Blocking Antibodies Targeting the CD39/CD73 Immunosuppressive Pathway Unleash Immune Responses in Combination Cancer Therapies. *Cell Rep* 2019;27:2411-2425.e9.

FIGURE LEGENDS

Figure 1. *CD39^{high}CD8^{+} T cells are accumulated in CRC and HNSCC cancers.*

(A-C) Representative FC analyses (A), and percentage of CD39^{high} or CD39^{dim} T cells in gated CD8^{+} T cells in PB, N-TUM and TUM districts, of CRC (N=35) and HNSCC (N=17) patients. * p <0.05, *** p < 0.001, **** p < 0 .0001, by Wilcoxon matched-pairs test, two-tailed. D-E) Percentage of CD39^{high} T cells in gated CD8^{+} T cells in PB, N-TUM and TUM districts of CRC (N=31) and HNSCC (N=15) patients according to the TNM classification (I-II stage *vs* III-IV stage). * p <0.05, by Student t-test.

Figure 2. *SNP rs10748643 A>G modulates CD39 expression on tumor-infiltrating CD8^{+} T cells.*

(A, B) Percentage of $CD39^+$ or $CD39^{high}$ cells in gated $CD8^+$ T cells in PB, N-TUM and TUM districts of GG homozygous CRC patients (N=5), as compared with the patients with AA and AG variants (N=30). * p <0.05, ** p<0.01, *** p <0.001, **** p <0.0001, by Wilcoxon matched-pairs test, two-tailed between districts (PB, N-TUM and TUM) and Mann-Whitney, two-tailed, between different genotypes. (C) Representative CD39/CD8 FC staining gated on $CD8^+$ T cells of 3 HDs, based on AA, AG or GG genotype at D0 and at D4, after 4 days of stimulation of PBMCs with anti-CD3 and anti-CD28 beads. The graph showed 1 representative experiment, out of 5 independent experiments. (D) Representative images from multiplex tissue immunofluorescence staining showing $CD8^+$ (white), $CD103^+$ (green), $CD39^+$ (red) T cells and nuclear staining with Hoechst (blue) in CRC lesions. 40x magnification. Triple $CD8^+CD103^+CD39^+$ T cells are indicated by arrows in magnification panels below each image (yellow); scale bars, 30 μm. Counts of tumor-infiltrating $CD8^+CD103^+CD39^+$ T cells from CRC (N=8) pts. * p< 0.05, by unpaired Student t-test, two-tailed.

Figure 3. *$CD39^+CD8^+$ T cells overexpress $PD1^+$ and produce low levels of IFN-γ, negatively correlating with cytotoxicity-related effector molecules*.

(A, B) Representative CD39/PD1 FC staining and percentage of $CD39^+PD1^-$, $CD39^+PD1^+$, $CD39^-PD1^+$, $CD39^-PD1^-$ in gated $CD8^+$ T cells in PB, N-TUM and TUM specimens of CRC pts (N=18). (C) Percentage of $PD1^+$ cells gated on $CD39^{high}$ or $CD39^{dim}$ $CD8^+$ T cells in PB, N-TUM and TUM specimens in CRC pts (N=26). *** p< 0.001, **** p<0.0001, by Wilcoxon matched-pairs test, two-tailed between districts (PB, N-TUM and TUM) and Student t-test, paired, between $CD39^{high}$ and $CD39^{dim}$. (D) Spearman correlation between percentage of

$CD39^{high}$ (N=32) and $PD1^+$ (N=31) $CD8^+$ T cells in N-TUM and TUM districts. * p<0.05. (E) Representative IFN-γ/CD45RA FC staining and percentage of IFN-γ^+ cells in gated $CD39^+$ and $CD39^-CD8^+$ T cells in PB, N-TUM and TUM specimens of CRC pts (N=11). * p<0.05 by Student *t*-test, paired. (F, G) Spearman correlation between the percentage of $CD39^+$ (N=36) and Granzyme-B^+ (N=18) or $Perforin^+$ (N=13) $CD8^+$ T cells. The correlation is calculated for pooled districts (PB, N-TUM and TUM); * p< 0.05 ** p< 0.01. (H) Percentage of IFN-γ^+ in gated $CD39^-PD1^+$, $CD39^+PD1^+$, $CD39^+PD1^-$, $CD39^-PD1^-CD8^+$ T cells in PB of a NSCLC patient at baseline (T0), and different times points (T1-T2-T3) upon Nivolumab (anti-PD1) treatment. Each treatment has been performed every 21 days.

Figure 4. *$CD103^+CD39^+$ CD8 T cells show lower IFN-γ and IL-2 production and higher PD1 expression than $CD103^+CD39^-$.*

(A) Representative IFN-γ, IL-2 and PD1/CD45RA FC staining and percentage of $PD1^+$ cells in gated $CD103^+CD39^-$ or $CD103^+CD39^+$ $CD8^+$ T cells in PB, N-TUM and TUM specimens of CRC pts (N=14). * p <0.05, ** p <0.01, *** p <0.001, by Wilcoxon matched-pairs test, two-tailed between districts (PB, N-TUM and TUM) and Student *t*-test, paired, between $CD103^+CD39^-$ and $CD103^+CD39^+$ CD8 T cells. (B) Spearman correlation between percentage of $CD103^+CD39^+$ (N=14) and $PD1^+$ (N=35) $CD8^+$ T cells in PB, N-TUM and TUM districts. ** p < 0.01.

Figure 5. *$CD39^+CD8^+$ T cells display high proliferative capacity and suppressive potential.*

(A) CFSE profile overlay and percentage of CFSE-diluting $CD39^+$ (violet) or $CD39^-$ (grey) $CD8^+$ T cells in PB, N-TUM and TUM specimens of one PCA patient out of 3 independent experiments. The percentage of CFSE-diluting cells in $CD39^+$ and $CD39^-$ CD8 T cells was evaluated at day 7 of culture of MCs with anti-CD3 and anti-CD28 (ratio 1:4). ** p <0.01 2way-ANOVA, Tukey's multiple comparison. (B) CFSE profile overlay and percentage of CFSE-diluting cells gated on $CD39^-PD\text{-}1^-$, $CD39^-PD\text{-}1^+$, $CD39^+PD\text{-}1^+$, $CD39^+PD\text{-}1^-$ (grey scale) in $CD8^+$ T cells in PB, N-TUM and TUM specimens of one PCA patient out of 3 independent experiments. The percentage of CFSE-diluting cells was evaluated in $CD39^-PD\text{-}1^-$, $CD39^-PD\text{-}1^+$, $CD39^+PD\text{-}1^+$, $CD39^+PD\text{-}1^-$ $CD8^+$ T cells at day 7 after culture of MCs with anti-CD3 and anti-CD28 (ratio 1:4). * p<0.05, ** p<0.01, *** p<0.001, 2way-ANOVA, Tukey's multiple comparison. (C) Percentage of $CD39^+$ cells gated on $CD8^+$ T cells and $Ki67^+$ in gated $CD39^+PD\text{-}1^+$, $CD39^-PD\text{-}1^+$, $CD39^+PD\text{-}1^-$, $CD39^-PD\text{-}1^-$ $CD8^+$ T cells in PB of a NSCLC patient upon Nivolumab (anti-PD-1) treatment at baseline (T0) and different times points (T1-T2-T3). Each treatment has been performed every 21 days. (D-E) Percentage of CFSE dilution (D) and percentage of inhibition (E) of CFSE dilution on gated $CD4^+$ T cells. The graph shows results of $CD39^+$ or $CD39^-$ sorted cells, labelled with eF670, after 4 days of co-culturing together with autologous PBMCs labelled with CFSE, at different ratios (1:1, 1:2, 1:4, 1:8, 1:16, 1:32, 1:64) and control autologous PBMCs cultured alone (1:0). The % of inhibition was calculated by the formula described in Material and Methods. The experiment was repeated thrice including 4 donors for each experiment and analysed in triplicates. * p< 0.05, ** p< 0.01, *** p< 0.001, **** p< 0.0001. 2way-ANOVA, Tukey's multiple comparison.

Figure 6. *POM-mediated inhibition of CD39 restores CD8$^+$ T cell effector functions in vitro and ex vivo.*

(A) Representative CD25, IFN-γ and CD107a/CD45RA FC staining in gated CD39$^+$CD8$^+$ T cells treated with 20 µM POM (left panel) or not (NT) and percentage of CD25$^+$, IFN–γ$^+$ and CD107a$^+$ cells gated on CD39$^+$ (white) and CD39$^-$ (grey) CD8$^+$ T cells in NT (medium alone), or POM-1 (20, 50 µM) conditions (right panel). PBMCs isolated from fresh blood of HD were stimulated with anti-CD3/anti-CD28 beads at a ratio 1:4 for 4 days in presence or absence of POM-1 (20 or 50 µM). The experiment was repeated four times and analysed in triplicates. * p<0.05, ** p< 0.01, **** p< 0.0001, 2way-ANOVA, Tukey's multiple comparison. Red statistic is calculated between CD39$^+$ and C39$^-$ subpopulations for each condition. (B-C) Percentage and mean fluorescence intensity (MFI) of CD107a and PD1 in gated CD8$^+$ T cells in PB, N-TUM and TUM of NT (medium alone) and POM-1 (20 µM) of CRC patients. Ex vivo assays were performed on MCs from PB, N-TUM and TUM, stimulated with anti-CD3/anti-CD28 beads (ratio 1:4) for 4 days. Cells were treated with POM-1 (20 µM) or medium alone (NT), once per day for 7 consecutive days. The experiment was repeated in 5 CRC patients. * p<0.05, ** p< 0.01, 2way-ANOVA, Tukey's multiple comparison. (D-E) Percentage and mean fluorescence intensity (MFI) of CD107a in CD8$^+$ T cells (D) and in gated CD39$^-$PD1$^+$, CD39$^+$PD1$^+$ and CD39$^+$PD1$^-$ (E) CD8$^+$ T cells. *Ex vivo* assays were performed on MCs from N-TUM and TUM of PCA patients (N=2), stimulated with anti-CD3/anti-CD28 beads (ratio 1:4) for 4 days. Cells were treated with POM-1 (20 µM) or medium alone (NT), once per day for 7 consecutive days. The panel E shows the analysis

of CD107a MFI on tumor-infiltrating MCs (TUM) of PCA patients. * $p<0.05$, ** $p< 0.01$, *** $p<0.001$, 2way-ANOVA, Tukey's multiple comparison.

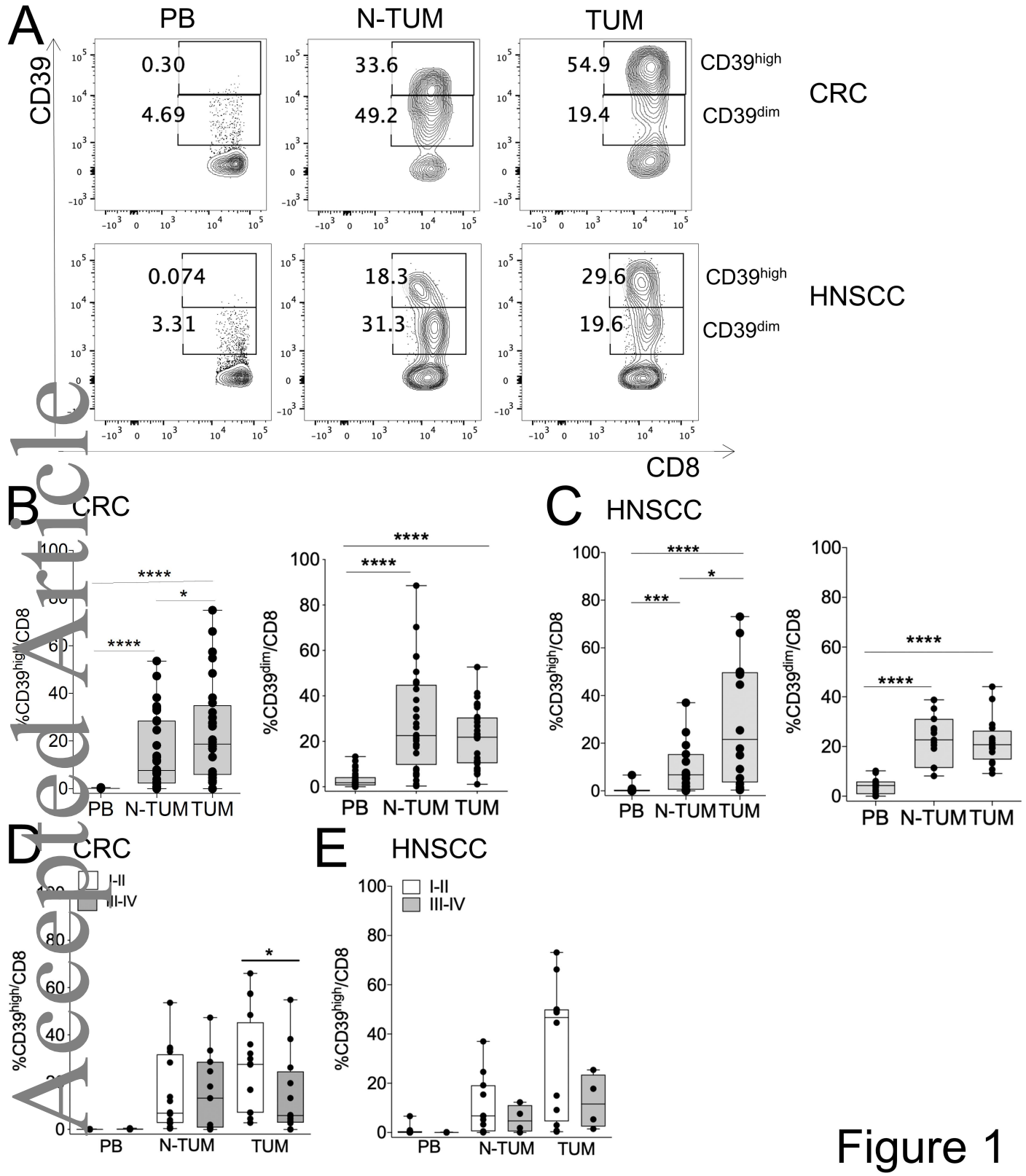

Figure 1

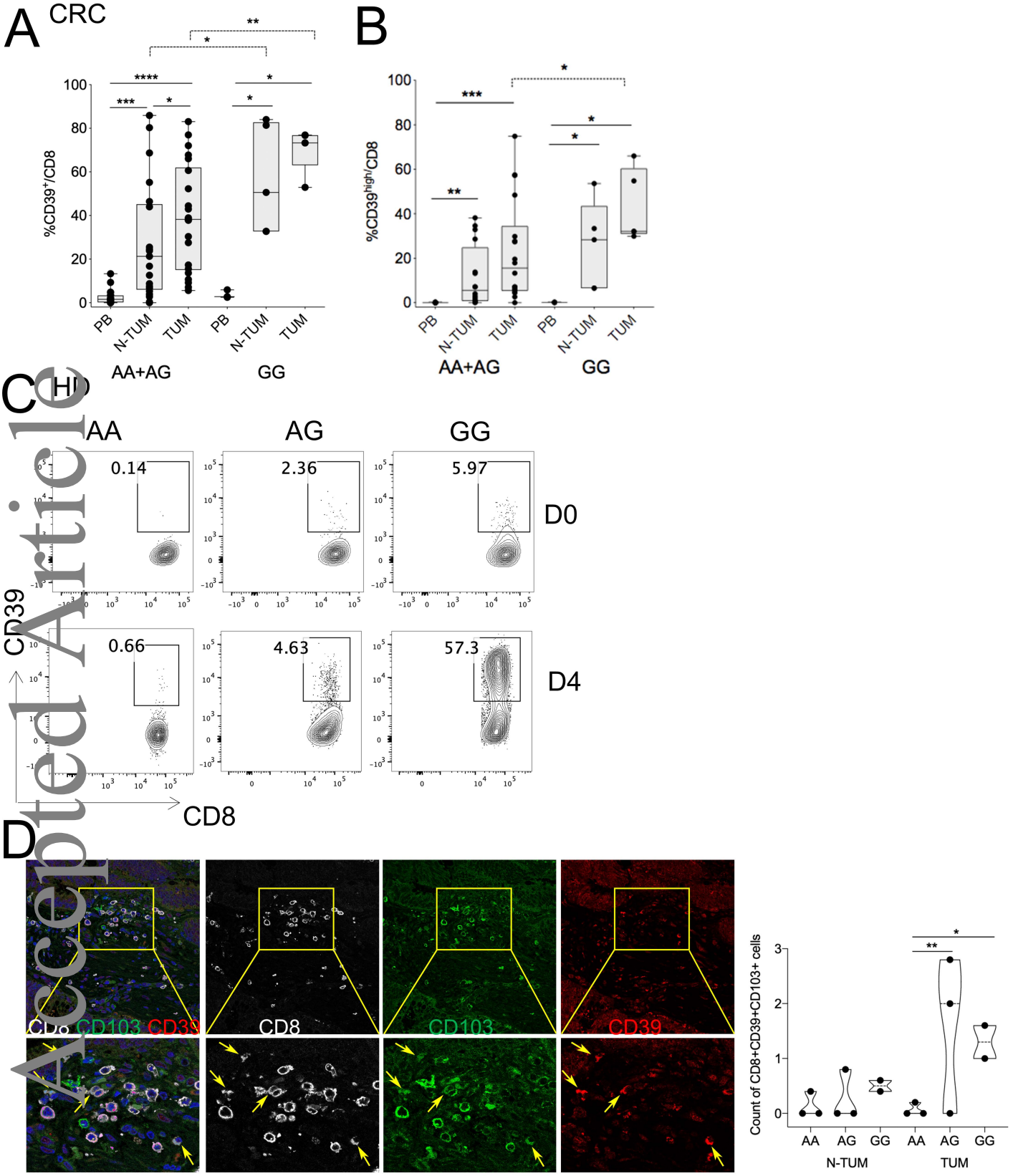

Figure 2

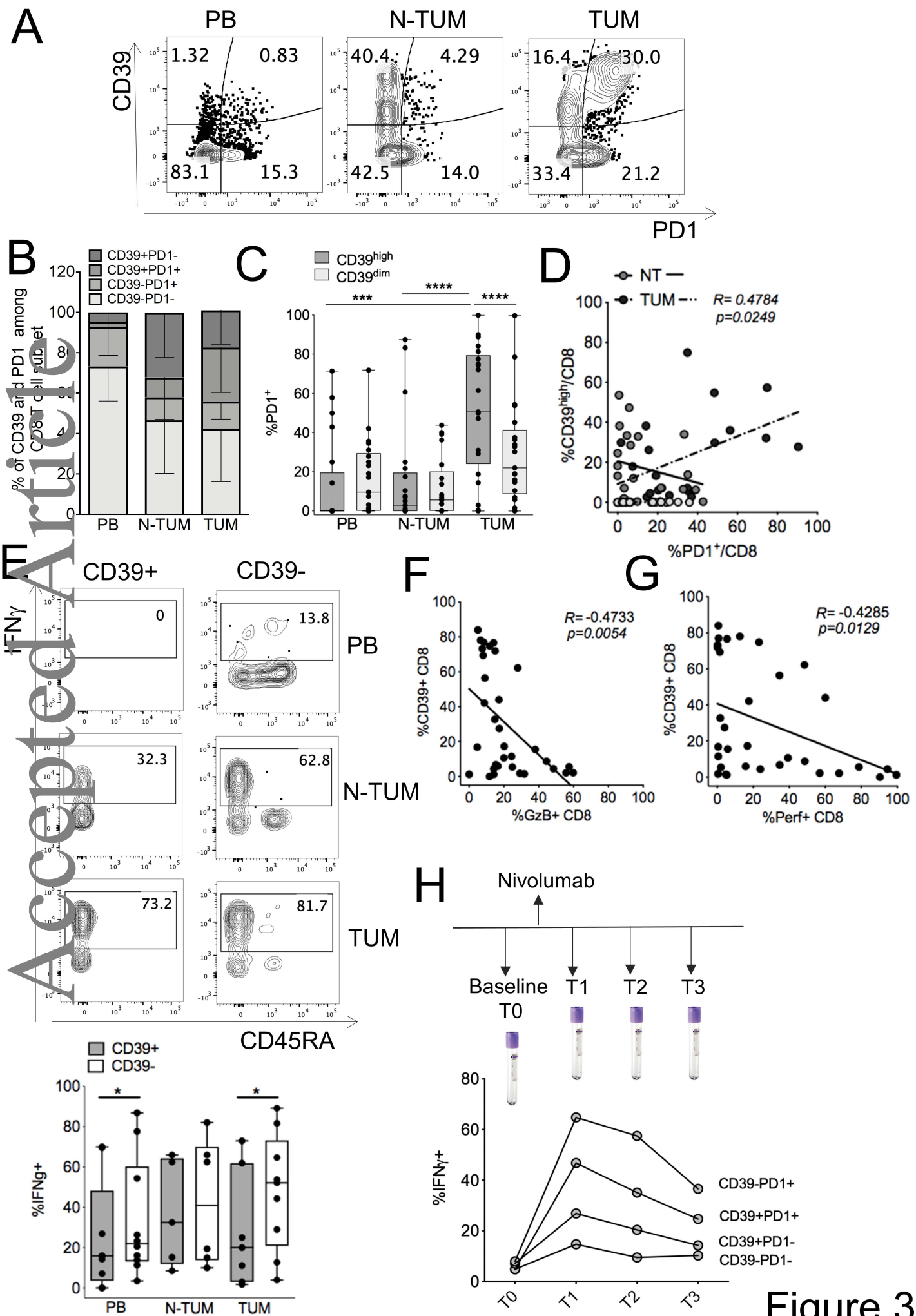

Figure 3

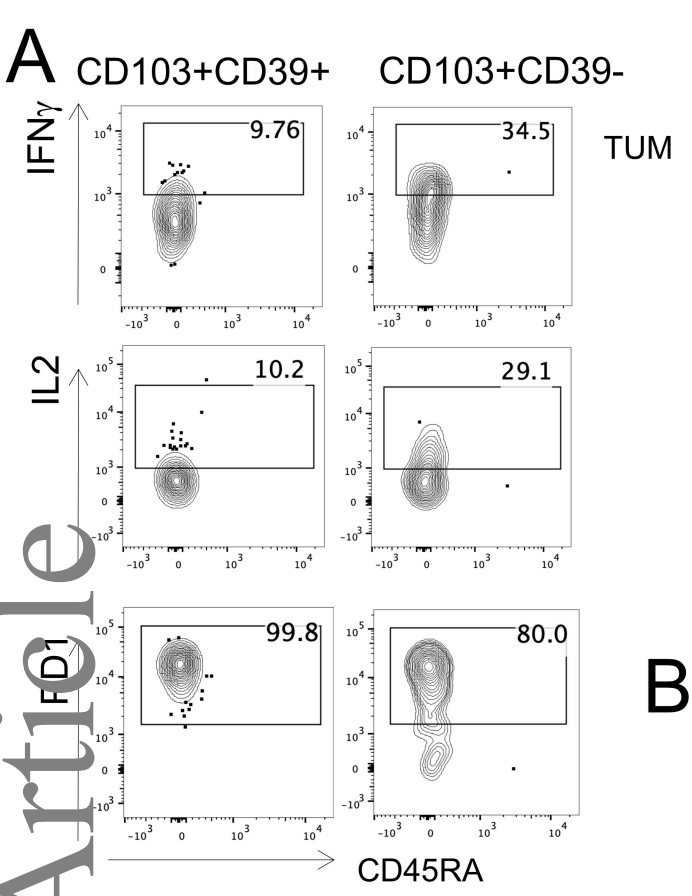

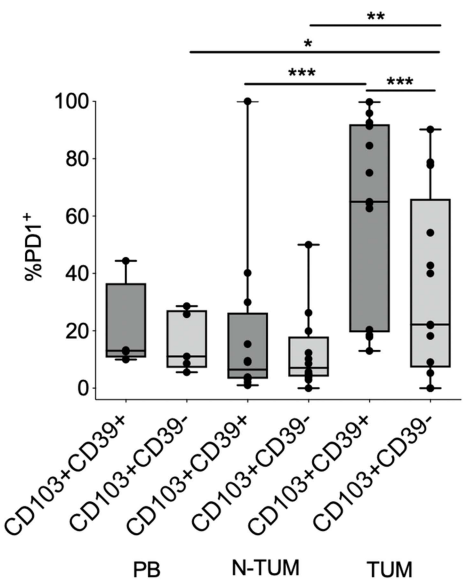

B

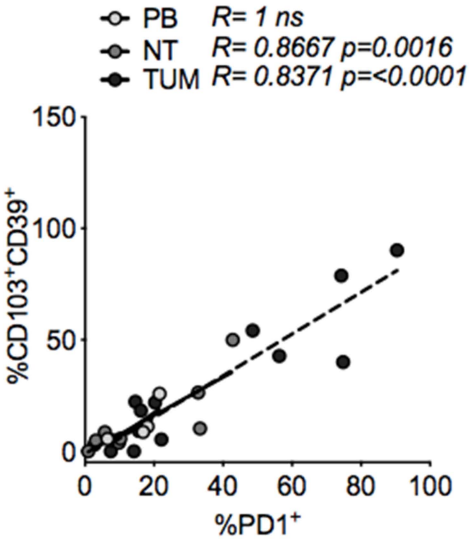

Figure 4

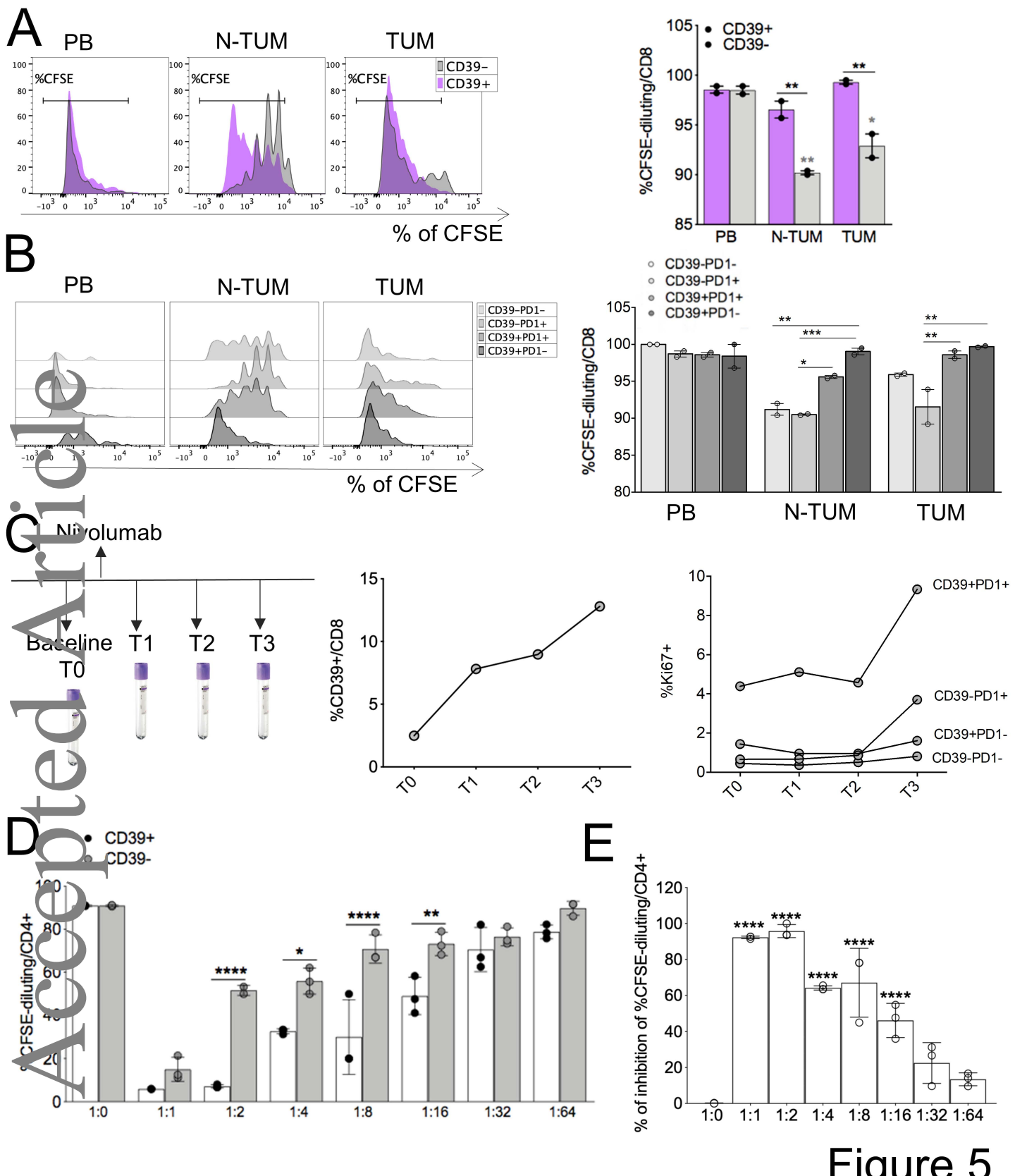

Figure 5

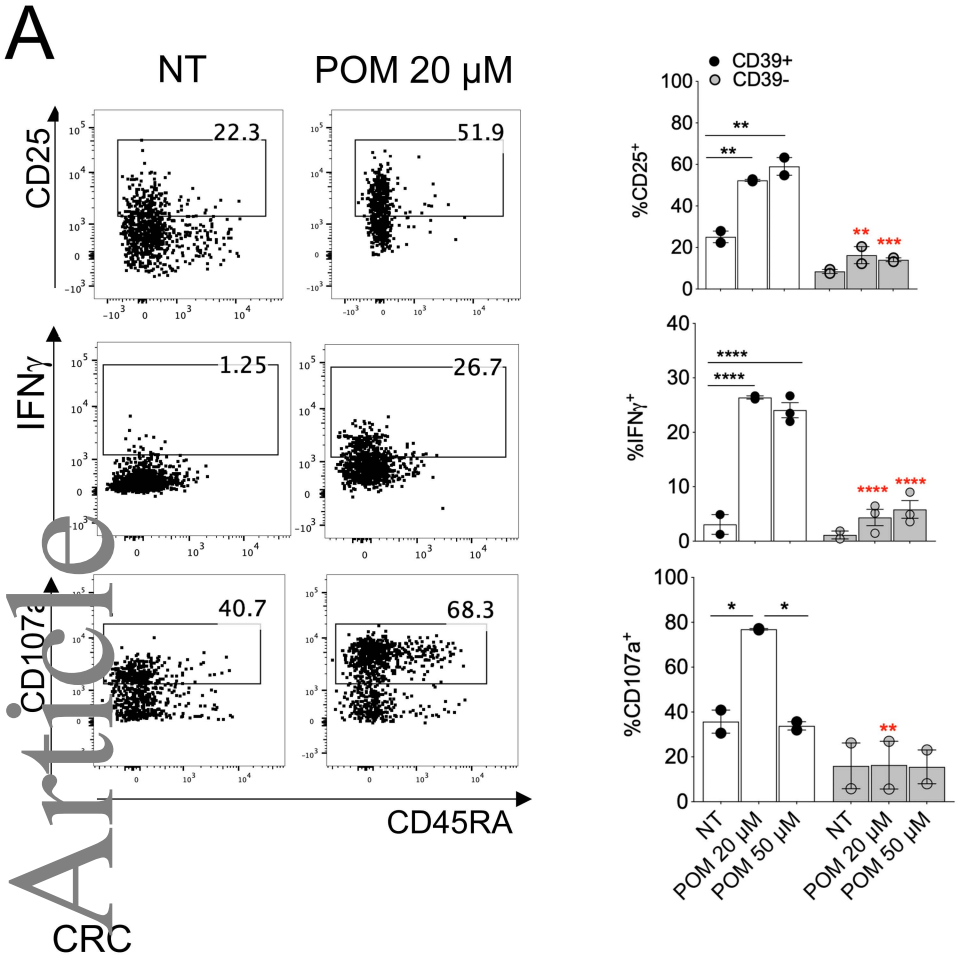

CRC

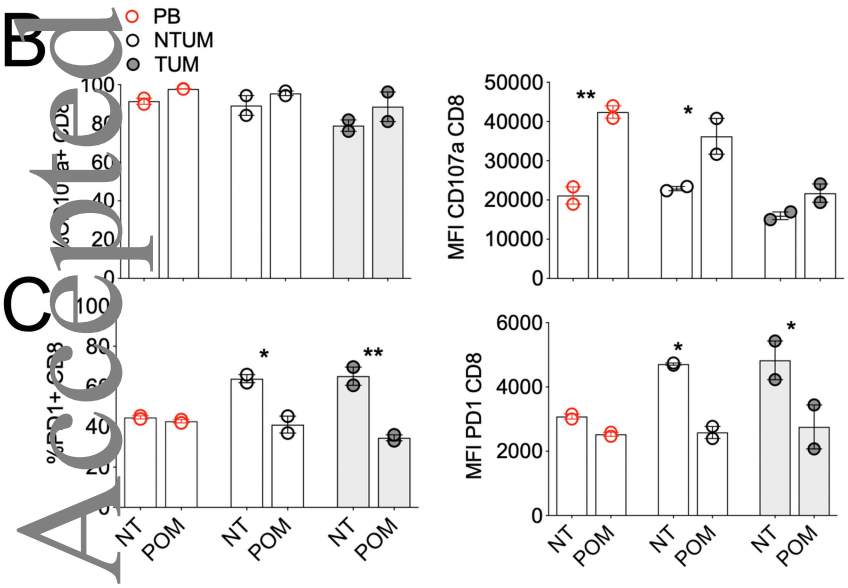

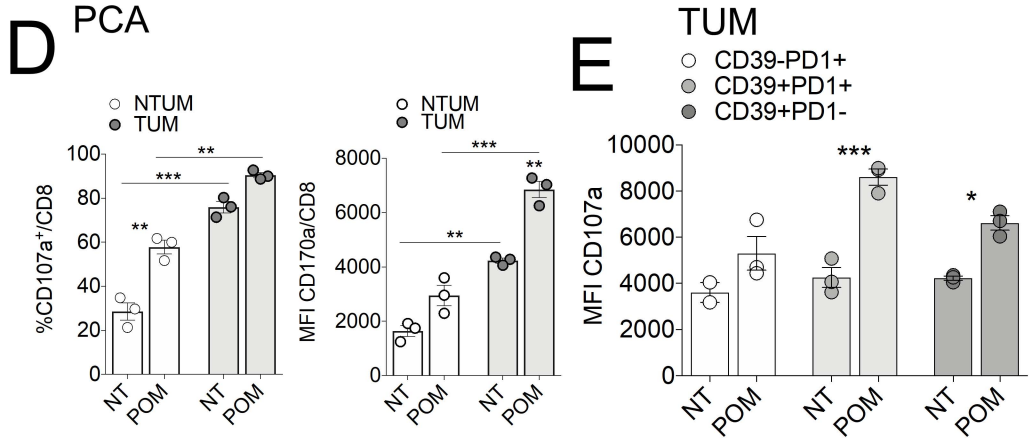

Figure 6